

# IMPLEMENTATION ASPECTS OF DOWNLINK MULTIUSER MIMO SYSTEM WITH DISTRIBUTED AND COHERENTLY-COORDINATED TRANSMIT ANTENNAS

Dragan Samardzija, Howard Huang, Clark Woodworth, Susan Walker, Reinaldo Valenzuela and Theodore Sizer

Alcatel-Lucent, Bell Laboratories,  
791 Holmdel-Keyport Road,  
New Jersey, 07733, USA

## ABSTRACT

*In this paper we present implementation aspects of a multi-user MIMO experimental system and the corresponding indoor measurement results that demonstrate power of distributed and coherently-coordinated downlink transmit antennas using zero-forcing (ZF) beamforming. We present functional partitioning between a DSP and FPGA platform and give implementation details and required resources. We demonstrate significant gains as well as moderate implementation requirements.*

## 1. INTRODUCTION

In the MIMO broadcast channel (MIMO-BC), a transmitter with multiple antennas sends information over a given bandwidth to multiple receivers. Recent works [1] have shown that the sum capacity of the MIMO-BC can be achieved by means of a nonlinear precoding technique at the transmitter known as *dirty paper coding* (DPC) [2]. Unfortunately, this technique has high computational complexity and is difficult to implement in practice.

Beamforming is a simpler, suboptimal technique where signals are simultaneously transmitted to multiple users on beams formed by weighting the phases and amplitudes of the transmitted signals. A particular type of beamforming known as zero-forcing (ZF) uses CSI at the transmitter to form non-interfering beams. It has been shown to achieve the sum-capacity of the MIMO-BC asymptotically as the number of users grows without bound and achieves a significant fraction of the DPC capacity for a finite number of users [3].

Typically, multiple transmit antennas are co-located at a base station so that beams formed by a given base are non-interfering (see [4] for experimental results). However, a user receiving a signal from the beam of one base may experience interference from another base's beam. Alternatively, one could perform ZF beamforming over antennas that are spatially distributed throughout the network. If CSI is known throughout the network for each user and the base stations transmit in a coordinated manner, then ideally the users would experience no intercell interference and the spectral efficiency would be greatly improved. A high-speed backhaul network would be required to connect the base stations. Either CSI would need to be transferred among base stations so that the ZF antenna weights are calculated locally at each base, or the CSI would

be transferred to a common point where ZF antenna weights are computed and then distributed to each antenna. Realistically, a fully coordinated macro-cellular network would require significant long-term planning. However, near-term applications could include an in-building pico-cell network or a limited outdoor area for hotspot coverage. These applications would be ideally suited for coordinated transmission since the need for spectral efficiency is high and the relatively short distances between base stations makes coordination feasible.

In this paper we present implementation aspects of an experimental system that was built for demonstrating ZF beamforming across spatially distributed antennas. Originally, the system was introduced in [5] focusing on the corresponding experimental results. In Section 2, we present the system model. In Section 3, we describe the experimental system implementation including the transmitter, receiver, and CSI feedback mechanism. In Section 4, we present some experimental results. We conclude in Section 5.

## 2. SYSTEM MODEL

We consider a narrowband multiantenna downlink channel modeled as a MIMO-BC with flat fading, where  $K$  users, i.e., mobile terminals, each equipped with a single receive antenna, request service from a transmitter with  $M$  distributed antennas. The discrete-time complex baseband received signal by the  $k$ th user is

$$y_k = \mathbf{h}_k \mathbf{x} + n_k, \quad k = 1, \dots, K \quad (1)$$

where  $\mathbf{h}_k \in \mathbb{C}^{1 \times M}$  is the  $k$ th user's channel vector,  $\mathbf{x} \in \mathbb{C}^{M \times 1}$  is the transmitted signal vector, and  $n_k \sim \eta(0,1)$  is the complex additive white Gaussian noise with zero mean and unit variance. The noise is uncorrelated among the users but the signal vector is the same for all users. Under zero-forcing beamforming, the transmitted vector  $\mathbf{x} = \mathbf{G}\mathbf{u}$  where  $\mathbf{u}$  is the  $K$ -dimensional information-bearing signal containing the modulation symbols for each user, and  $\mathbf{G} = \mathbf{H}^H (\mathbf{H}\mathbf{H}^H)^{-1}$  is the  $M \times K$  beamforming matrix where  $\mathbf{H} = [\mathbf{h}_1^H \ \mathbf{h}_2^H \ \dots \ \mathbf{h}_K^H]^H$  is the  $K \times M$  channel matrix. Note that we assumed that the transmitter has perfect knowledge of the CSI. In this case, we can rewrite the received signal by the  $k$ th user in (1) as  $y_k = u_k + n_k$ ,  $k = 1, \dots, K$ . Hence the rate achieved by this user is simply  $\log_2(1 + \nu_k)$ , where  $\nu_k = E[|u_k|^2]$  is the power allocated to the

$k$ th user. The transmit power at the  $m$ th antenna is  $\sum_{k=1}^K |\mathbf{G}_{mk}|^2 v_k$ . Hence the sum rate optimization subject to a transmit power constraint  $P_m$  on the  $m$ th antenna can be written as:

$$\begin{aligned} & \max_{v_1, \dots, v_K} \sum_{k=1}^K \log(1 + v_k), \text{ subject to} \\ & \begin{cases} v_k \geq 0, k = 1, \dots, K \\ \sum_{k=1}^K |\mathbf{G}_{mk}|^2 v_k \leq P_m, m = 1, \dots, M \end{cases} \end{aligned}$$

This optimization has been shown to be a convex optimization [3] which can be solved using conventional interior point techniques.

### 3. EXPERIMENTAL SYSTEM

The experimental system that is used in this study is depicted in Fig. 1. It consists of  $M = 4$  distributed downlink transmit antennas and  $K = 2$  mobile terminals, each with a single receive antenna. The transmit antennas are connected to the outputs of the beamformer. The beamformer resides in a base station that determines its coefficients and applies them on the information-bearing signals for each mobile terminal. Using a pilot-assisted channel state estimation, the mobile terminals estimate the downlink channel states between each transmit and receive antenna. The quantized estimates, that correspond to channel state information (CSI), are fed back to the base station, where they are used to determine the beamforming coefficients.

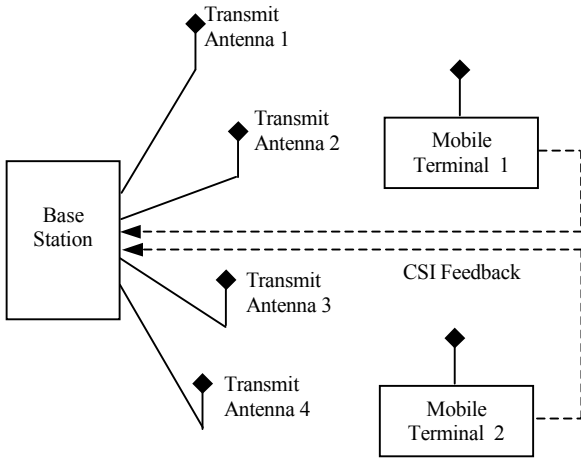


Fig. 1: Experimental system overview.

#### Base Station

The functional block diagram of the base station is presented in Fig. 2. The base station receives CSI from the mobile terminals. Specifically, mobile terminal  $k$  feeds back estimates of the  $k$ th row vector of the MIMO channel matrix  $\mathbf{H}$  (for  $k = 1, 2$ ). Having the CSI received, the base station determines the beamforming coefficients.

The output of the generalized beamformer is  $\mathbf{x} = \mathbf{G}\mathbf{u}$ , where  $\mathbf{x} \in \mathbb{C}^{4 \times 1}$  and  $\mathbf{G} \in \mathbb{C}^{4 \times 2}$  is the beamforming matrix. Further-

more,  $\mathbf{u} \in \mathbb{C}^{2 \times 1}$  is the input vector where  $u_k$  is its  $k$ th element and it corresponds to the signal dedicated to mobile terminal  $k$  ( $k = 1, 2$ ). The signal  $u_k$  consists of the information-bearing signal as well as dedicated pilot  $k$  (i.e., reference signal). Dedicated pilot  $k$  allows the mobile terminals to estimate the  $k$ th column entries of the composite MIMO channel matrix  $\mathbf{H}\mathbf{G}$ . The particular estimates are used by the mobile terminals to perform coherent detection of the information bearing portion of the signal  $u_k$  (for  $k = 1, 2$ ) without any explicit knowledge of beamforming that is performed by the base station. To simplify the estimation procedure, the dedicated pilots are orthogonal in signal space to the information-bearing portion of the signals, and to each other.

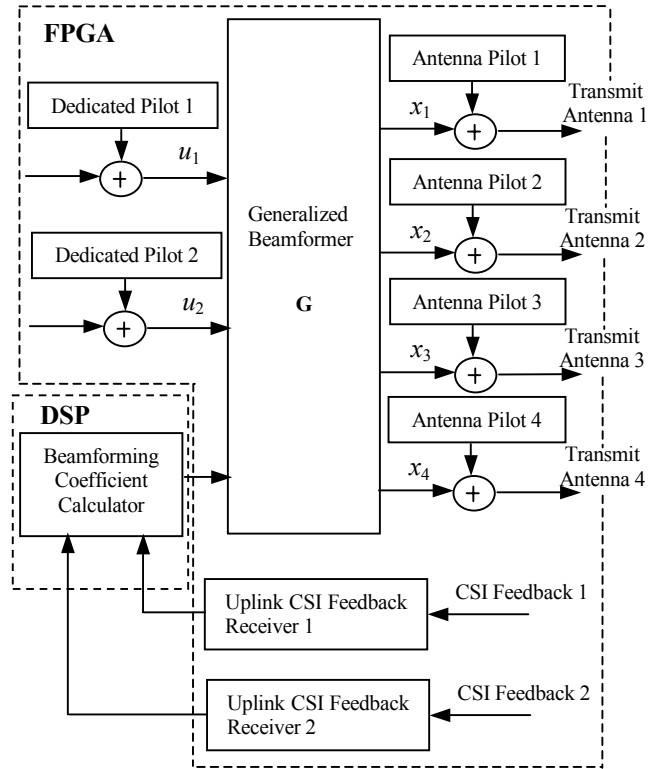


Fig. 2: Base station functional blocks.

Before being transmitted over the corresponding downlink transmit antenna, a unique pilot is added to each beamformer outputs. The antenna-specific pilots allow mobile terminals to perform pilot-assisted estimation of the MIMO channel  $\mathbf{H}$ . Specifically, mobile terminal  $k$  estimates the  $k$ th row vector of the matrix  $\mathbf{H}$ . The quantized estimates correspond to the CSI that is fed back to the base station. To simplify the estimation procedure, the antenna-specific pilots are orthogonal in signal space to the beamformer outputs and to each other.

The most of the functional blocks that are depicted in Fig. 2 are implemented on a FPGA platform (Xilinx Virtex II 6000), using a small fraction of the available resources. Only the beamformer coefficient calculator is implemented on a floating point DSP (TI 6701).

The FPGA resources are mostly taken by the beamformer. The beamformer coefficients have a 32-bit resolution (16 bits for real and 16 bits for imaginary component). Similarly, its inputs and outputs have the same resolution. The required FPGA resources are presented in Table 1. The number of used embedded multipliers is equal to the number of multiplications needed to perform ZF beamforming, which is  $N_{mult} = 2KM$ . Note that the Virtex II family features 18-bit embedded multipliers.

	Used	Available	Utilization
Number of slice flip flops	3,160	67,584	4%
Number of occupied slices	2,692	33,792	7%
Number of Block RAMs	6	144	4%
Number of embedded 18-bit multipliers	16	144	11%

**Tab. 1:** Base station FPGA resources (Virtex II 6000).

The beamformer and pilot generators logic operates at 1.2288 MHz, resulting in a low-power solution.

The FPGA is a part of the DSP memory map. The received CSI that is fed back from the mobile terminals is stored in the FPGA, and accessed by the DSP. The DSP performs the channel matrix inversion, i.e., it calculates  $\mathbf{G} = \mathbf{H}^H(\mathbf{H}\mathbf{H}^H)^{-1}$  and power allocation. The inversion algorithm is implemented using the DSP floating-point arithmetic. The matrix  $\mathbf{G}$  is calculated whenever a new CSI is received (for example, once in 2.08332 msec, as in the experiments that are presented in the following section). The resulting entries of the matrix  $\mathbf{G}$  are linearly quantized and stored back in the FPGA. The FPGA applies them as the beamformer coefficients.

### Mobile Terminal

The functional block diagram of the mobile terminal is presented in Fig. 3. It consists of a number of estimators that implement *maximum likelihood* estimation. Specifically, in this implementation the mobile terminal functionality is dedicated to assessing the performance of the distributed antenna beamforming.

The estimators that correspond to dedicated pilot 1 and 2 are used to estimate the received power of the signal that is dedicated to mobile terminal 1 and 2, respectively.  $\hat{S}_{kl}$  denotes estimated power of mobile terminal  $l$  signal that is received at mobile terminal  $k$ . For example, in the case when idealized ZF beamforming and estimation are applied, the received power estimates should be  $\hat{S}_{12} = \hat{S}_{21} = 0$  with  $\hat{S}_{11} \geq 0$  and  $\hat{S}_{22} \geq 0$ , which is a direct consequence of the zero-forcing criterion.

As a figure of merit we consider signal-to-noise-plus-interference ratio (SINR)

$$\text{SINR}_1 = \frac{\hat{S}_{11}}{\hat{S}_{12} + \hat{N}_{10}} \quad \text{and} \quad \text{SINR}_2 = \frac{\hat{S}_{22}}{\hat{S}_{21} + \hat{N}_{20}}$$

where  $\hat{N}_{10}$  and  $\hat{N}_{20}$  are estimates of the noise power at mobile terminal 1 and 2, respectively.

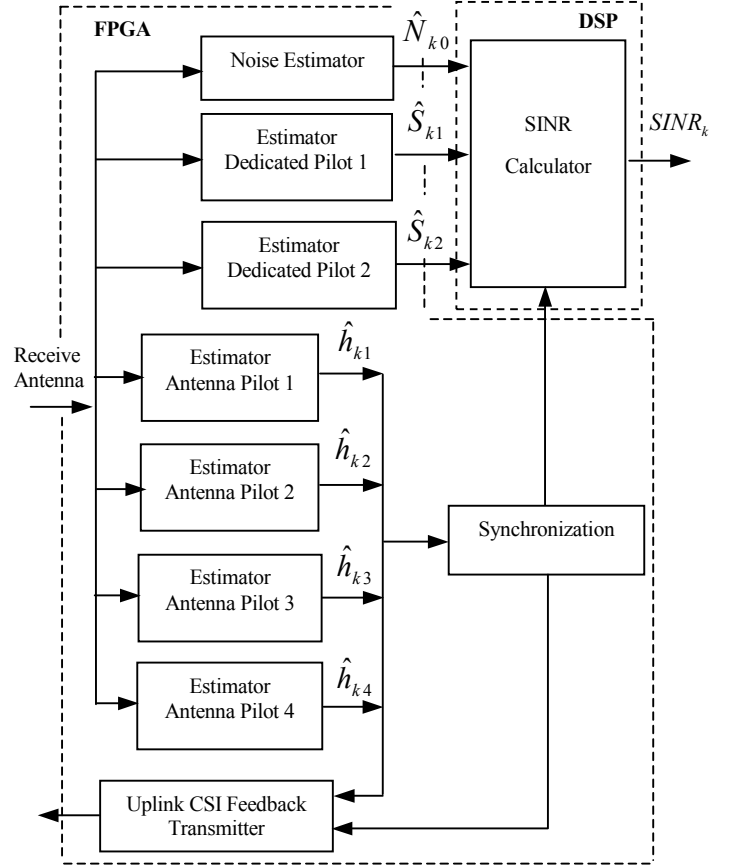


**Fig. 3:** Mobile terminal functional blocks,  $k = 1$  or  $2$ .

The antenna-specific pilots are used by the mobile terminals to perform pilot-assisted estimation of the MIMO channel  $\mathbf{H}$ . As said earlier, mobile terminal  $k$  estimates the  $k$ th row vector  $\hat{\mathbf{h}}_k = [\hat{h}_{k1} \dots \hat{h}_{k4}]$  of the matrix  $\mathbf{H}$ . The quantized estimates correspond to the CSI that is transmitted back to the base station, where is used to calculate the beamforming coefficients.

The most of the functional blocks that are depicted in Fig. 3 are implemented on the FPGA platform (Xilinx Virtex II 6000). Only the SINR calculator is implemented on the floating point DSP (TI 6701).

Each estimator is a sliding correlator, correlating the received signal against a particular reference pilot symbol sequence. They operate at 61.44 MHz. The reference pilot sequences are bipolar, allowing for significant simplification of the estimators implementation. Specifically, no explicit multiplication is required.

The input to the estimators has 8-bit resolution per each complex component. In addition the synchronization is based on the peak sum power detector of the estimators' outputs. The summary of the required FPGA resources is given in Table 2.

	Used	Available	Utilization
Number of slice flip flops	19,606	67,584	29%
Number of occupied slices	16,930	33,792	50%
Number of Block RAMs	0	144	0%
Number of embedded 18-bit multipliers	8	144	5%

**Tab. 2:** Mobile terminal FPGA resources.

The SINR calculator is implemented as a monitoring quasi-real-time application on the DSP. The DSP reads the memory-mapped outputs of the estimators and calculates the SINR and other related quantities. The SINR traces are presented within the PC-based DSP integrated development environment CodeComposer.

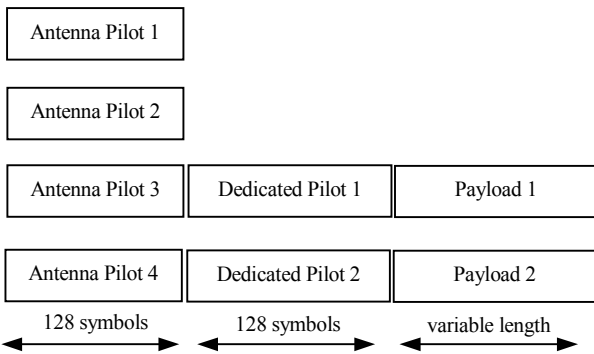


**Fig. 4:** Temporal relationship between the antenna-specific pilots, dedicated pilots and the payloads.

### Signal Arrangement

The symbol rate of the experimental system is set to 1.2288 Msym/secs, which is identical to the cdma2000/EV-DO chip rate.

The antenna-specific pilots span 128 symbols, lasting 104.166 usec, and they are code-multiplexed. The dedicated pilots have the identical duration and multiplexing scheme. The pilot codes are mutually orthogonal and random with a low cross correlation. Immediately after the antenna-specific pilots, the dedicated pilots are transmitted. Furthermore, the information-bearing portion (payload) of the signal follows after the dedicated pilots. The payload duration may vary depending on a particular experimental setup. The temporal relationship between the pilots and the payloads is depicted in Fig. 4.

Note that the beamforming is *not* performed while the antenna-specific pilots are being transmitted. The beamforming is applied during the transmission of the dedicated pilots and payloads.

### Channel State Information Feedback

Mobile terminal  $k$  periodically obtains the channel state estimates  $\hat{\mathbf{h}}_k = [\hat{h}_{k1} \dots \hat{h}_{k4}]$ , ( $k = 1, 2$ ).

The shortest period between new estimates is 256 symbols, i.e., 208.332 usec. The shortest period corresponds the case when no payload is transmitted.

Before being transmitted on the uplink, each component of the vector  $\hat{\mathbf{h}}_k$  is quantized with a 15-bit liner quantizer both for the real (I) and imaginary (Q) component.

The CSI feedback channel is realized over a cable (CAT5), which is a highly controllable medium allowing us to assess the system performance under different CSI feedback channel conditions. The uplink CSI feedback transmitter and receiver are built around the Xilinx low-voltage differential signalling (LVDS) output and input ports, with 122.88 MHz and 61.44 MHz clocks, respectively.

### Analog Front-End

The base station front-end consists of four UMTS/HSDPA radio cards that are a part of the multi-standard Lucent commercial base station OneBTS. The digital-to-analog interface is of 16-bit resolution per each complex component. The radio transmitter features exceed the 3GPP HSDPA error vector magnitude (EVM) requirements.

The mobile terminal front-end is based on a heterodyne architecture, followed by a 10-bit analog-to-digital converter, where 8 most significant bits are used as the estimators' inputs. The carrier frequency is set to 2.1 GHz.

Furthermore, the downlink transmitters and each mobile terminal have free running oscillators that are manually tuned. The measured frequency offsets and clock drifts are negligible compared to the estimation periods and wireless channel coherence periods.

## 4. EXPERIMENTAL RESULTS

The experimental results that are presented in this section are based on the measurements that are conducted in our laboratory. The laboratory floor plan is given in Fig. 5, where the solid lines correspond to its walls. Typical laboratory furniture (benches and wooden cabinets), computers and instruments occupy the laboratory, thus, creating a rich scattering environment. Each downlink transmit antenna (TX1 to TX4) is placed close to a different corner of the laboratory. The exact positions of the transmit antennas are given in Fig. 5. The height of each transmit antennas is 2 m. During the measurements, the mobile

terminals (M1 and M2) are placed randomly within the shaded region in Fig. 5. Per each measurement setup, 100 SINR measurements are recorded each corresponding to different positions of mobile terminal 1 and 2.

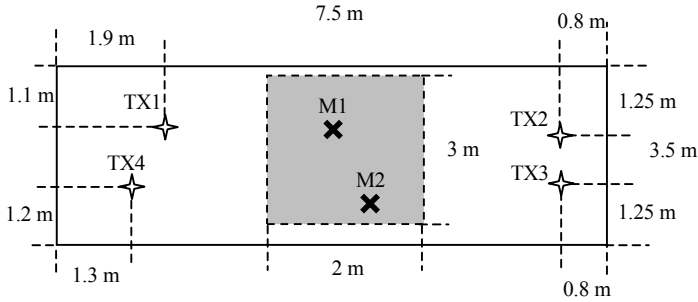


Fig. 5: Laboratory floor plan.

For the results that are presented in this section, the CSI is fed back every 2.08332 msec (480 times per second), corresponding to 5% overhead for the antenna-specific pilots as well as 5% overhead for the dedicated pilots. Furthermore, if not stated otherwise, the 15-bit linear quantizer is used for the real (I) and imaginary (Q) component of the channel state estimate.

In all cases the total average transmit power is identical. For example, in a case when the number of transmit antennas is  $M = 4$  the average transmit power per one antenna is 4 times lower than in a case with the single transmit antenna,  $M = 1$ .

The CDF of the measured achievable downlink sum data rates is presented in Fig. 6. In addition to ZF beamforming that is described in the previous sections, we present a single user case. In the single user case, the information-bearing signal is sent only to one of the users. The signal is sent from transmit antenna 1 (TX1). The single user case would correspond to a time-division multiplexing where transmissions for different users are orthogonalized in time. Furthermore, we considered a case when no beamforming is applied. Specifically, the information-bearing signal for mobile terminal 1 is transmitted only from transmit antenna 1 (TX1). Concurrently, the information-bearing signal for mobile terminal 2 is transmitted only from transmit antenna 2 (TX2). In other words, two independent transmissions are happening at the same time without any interference mitigation scheme being applied. The rates account for the pilot overhead. The pilot overhead for ZF beamforming is 10% while for the other two schemes it is 5% (because the antenna-specific pilots are not needed). The results demonstrate significant gains for ZF beamforming.

In Fig. 7 CDF of measured SINR is presented for different resolutions of the CSI quantizer and ZF beamforming (for  $M = 4$  and  $K = 2$ ). Considering that the CSI is fed back every 2.0833 msec, the presented 15-, 8-, 6- and 4-bit quantizer correspond to the CSI feedback data rates of 57.6 kbps, 30.72 kbps, 23.04 kbps and 15.36 kbps, respectively. Note that the applied quantizer is linear and not optimal.

A detailed report on experimental results can be found in [5].

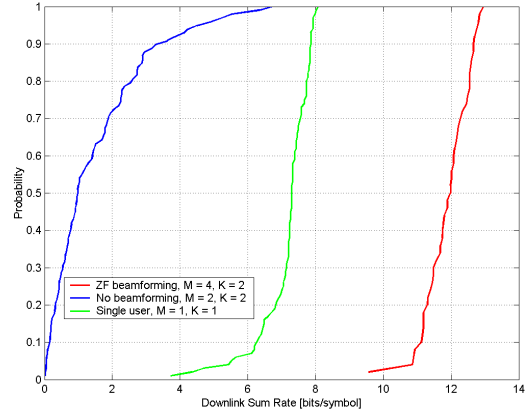


Fig. 6: CDF of measured downlink sum data rates for different transmission schemes.

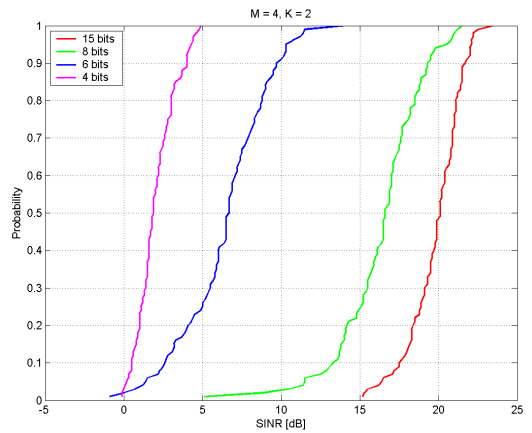


Fig. 7: CDF of measured SINR for different resolution of the CSI quantizer.

## 5. CONCLUSION

We have presented the implementation aspects of the multi-user MIMO experimental system. We have reported some experimental results. Furthermore, we have demonstrated significant gains for ZF beamforming as well as moderate implementation requirements.

## REFERENCES

- [1] H. Weingarten, Y. Steinberg, S. Shamai, "Capacity region of the MIMO broadcast channel," *IEEE Trans. Inform. Theory*, vol. 52, no. 9, pp. 3936-3964, September 2006.
- [2] M. Costa, "Writing on dirty paper," *IEEE Trans. Inform. Theory*, vol. 29, no. 3, pp. 439-441, May 1983.
- [3] F. Boccardi, H. Huang, "Zero-forcing precoding for the MIMO broadcast channel under per-antenna power constraints," *IEEE Workshop on Signal Processing Advances in Wireless Communications*, July 2006.
- [4] T. Haustein, A. Forck, H. Gaebler, C.v. Helmolt, V. Jungnickel, U. Krueger, "Implementation of adaptive channel inversion in a real-time MIMO system," *IEEE PIMRC*, September 2004.
- [5] D. Samardzija, H. Huang, R. Valenzuela, T. Sizer, "An experimental downlink multiuser MIMO system with distributed and coherently-coordinated transmit antennas," *IEEE ICC*, June 2007.